2024 European Control Conference (ECC)
June 25-28, 2024. Stockholm, Sweden

# Connecting Disconnected Agents in Multiagent Systems via Federated Control

Rongrong Qian, Zhisheng Duan, Yuan Qi, Tao Peng, and Wenbo Wang

Abstract— This study develops a control technique, called federated control, to connect disconnected agents in multiagent systems aided by control stations. Specifically, we first use a federated architecture to model multiagent systems with control stations. Based on this architecture, a federated-control procedure is proposed for the task of connecting disconnected agents, together with an initialization procedure. Then, how the federated-control procedure connects disconnected agents by incorporating simple global coordination (i.e., global averaging) is analyzed. We derive the close-form expression of the time sufficient to connect disconnected agents, which possesses interesting properties including early computability and delay independence. The convergence of the formation of multiagent systems and the velocities of all agents can also be proved.

## I. Introduction

Network connectivity has been in the focus of researchers of multiagent systems [1]–[8], since it is of vital importance to the collective behavior coordination of these systems [3], [4], [9]. Pioneering works are generally concerned with estimating, preserving, and increasing the network connectivity [1]–[9]. Most existing studies of multiagent systems adopt the all-time [1]–[8] or intermittent connectivity assumption [9], [10] which implies that a multiagent system can maintain its communication graph connected at all times or "intermittently connected infinitely often" during the evolution of the system. From a practical point of view, both all-time connectivity and intermittent connectivity might be restrictive requirements for multiagent systems due to the limited communication capabilities and motions of agents [11], [12].

Nevertheless, few existing studies consider network-disconnected systems in which neither all-time connectivity nor intermittent connectivity is assured, while the network disconnected problem have to be taken into account [11], [12], since there is no absolute guarantee that a realistic multiagent system will never be disconnected especially when the systems are initializing or experiencing severe failures [11], [12]. Our previous work [12] provided a technique of identifying disconnected agents for multiagent systems via external estimators in control stations[1]; however, the problem of connecting disconnected agents has not yet been addressed. Besides, multiagent systems could be highly autonomous from a technical perspective, but for reasons such as public safety, they must operate under human supervision at control stations in most situations, and will require human regulation on many occasions [12], [14].

In fact, a multiagent system with a control station can be modeled using the federated architecture that originates from the distributed computing of "federated learning" and is also named the server-agent architecture [15]–[19]. After emerging in distributed computing research, the federated architecture has shown its broad

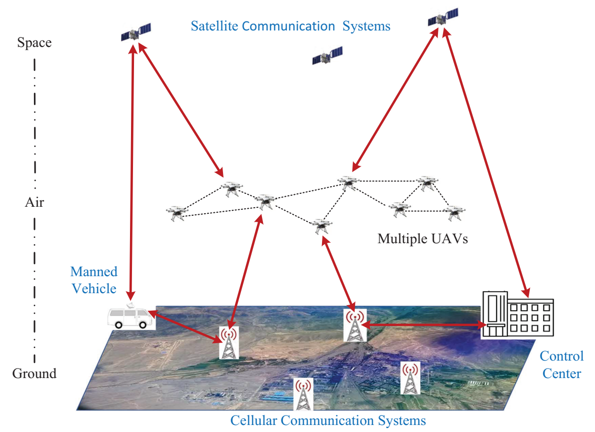


Fig. 1. As the space-air-ground integrated network is gradually being built [13], ground control centers and manned vehicles can serve as control stations that supervise and regulate multiagent systems including systems of multiple unmanned aerial vehicles (UAVs).

R. Qian is with the School of Artificial Intelligence, Beijing University of Posts and Telecommunications (BUPT), Beijing 100876, China (e-mail:rongrongqian@bupt.edu.cn).

Z. Duan is with the State Key Laboratory for Turbulence and Complex Systems, College of Engineering, Peking University, Beijing 100871, China (e-mail:duanzs@pku.edu.cn).

Y. Qi is with the School of Electronic Engineering, Beijing University of Posts and Telecommunications (BUPT), Beijing 100876, China (e-mail:qiyuan@bupt.edu.cn).

T. Peng and W. Wang are with the Wireless Signal Processing and Network Lab (Key Lab. of Universal Wireless Communication, Ministry of Education), Beijing University of Posts and Telecommunications (BUPT), Beijing 100876, China (e-mail:pengtao@bupt.edu.cn;wbwang@bupt.edu.cn).

[1]The control station can be a ground control center or a manned vehicle [12], see Fig. 1 for illustration. In the context of the space-air-ground integrated network [13], cellular and satellite communication systems facilitate the connections between control stations and multiagent systems.

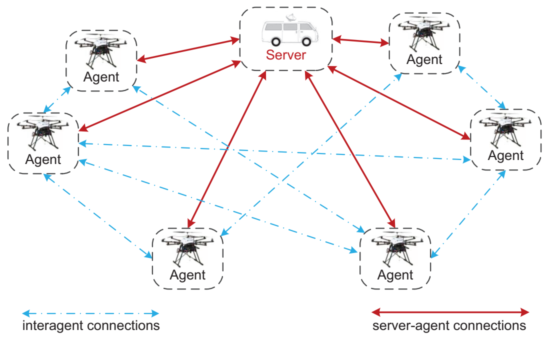


Fig. 2. The federated architecture for a multiagent system with a control station, e.g., a manned vehicle, that acts as a server. Although the communication over a server-agent connection has a high overhead [12], the number of server-agent connections is relatively small in a federated architecture.

applicability in machine learning [15], signal processing [16], communications [17], control [18], and optimization [19]. Note that our recent study [20] applied the federated architecture-based strategy to the design of compressive sensing algorithms. As we will see in this paper, the federated architecture can be applied to model multiagent systems with control stations, giving rise to a control technique referred to as federated control for connecting disconnected agents.

These facts motivate the study to be presented in this paper. In this study, we develop a federated-control technique for connecting disconnected agents in multiagent systems aided by control stations, which consists of federated-control and initialization procedures. We derive the close-form expression of the time sufficient to connect certain pair of disconnected agents (Theorem 1). Two important aspects of this expression are that, i) it can be computed in the initialization procedure and allows the control stations, at the initialization procedure, to know when the task of connecting disconnected agents will be accomplished (i.e., the task-time early computability stated in Remark 1), and ii) its value is delay independent (Remark 4). The convergence of multiagent systems can also be proved (Corollary 1 and Theorem 2). To the best of authors' knowledge, this study is the first to provide self-contained design and analytical frameworks for federated control of multiagent systems, with the aim of developing a technique to connect disconnected agents in multiagent systems aided by control stations.

## II. Model

In this section, we introduce a control technique, i.e., federated control, which can be used for multiagent systems aided by control stations.

### A. Federated Control

We consider a multiagent system that has $N$ agents moving in $\mathbb{R}^M$ space, with first-integrator dynamics

$$\dot{\boldsymbol{p}}_i(t) = \boldsymbol{u}_i(t), \quad t \geq 0, \tag{1}$$

where $\boldsymbol{p}_i(t) \in \mathbb{R}^M$ is the position vector of agent $i$, $i = 1, \cdots, N$, and $\boldsymbol{u}_i(t) \in \mathbb{R}^M$ denotes the control input. There exists a control station for supervising and regulating the multiagent system [12], [14], which plays the role of a server. A federated (server-agent) architecture can thus be built, see Fig. 2. Based on the federated architecture, we propose the following procedure for connecting disconnected agents, as well as for achieving a desired formation.

Federated-Control Procedure. It consists of two steps, starting from $t = 0$:

1) Every agent $i$ computes

$$\boldsymbol{x}_i(t) = \boldsymbol{p}_i(t) - \boldsymbol{\delta}_i - \boldsymbol{v}^* t, \quad t \geq 0, \tag{2}$$

and transmits $\boldsymbol{x}_i(t)$ to the sever, where $\boldsymbol{\delta}_i \in \mathbb{R}^M$ is the desired position within the formation, and $\boldsymbol{v}^* \in \mathbb{R}^M$ is the desired velocity. The sever then averages all values of $\boldsymbol{x}_i(t)$ to obtain

$$\overline{\boldsymbol{x}}\left(t\right) = \frac{1}{N} \sum_{l=1}^{N} \boldsymbol{x}_i\left(t\right), \tag{3}$$

and broadcast $\overline{\boldsymbol{x}}\left(t\right)$ to all the agents.

2) After obtaining $\overline{\boldsymbol{x}}\left(t\right)$, every agent $i$ uses the control law below

$$\begin{aligned}\boldsymbol{u}_i(t) = \boldsymbol{v}^* - \theta \sum_{j=1}^{N} g_{ij}\left(t\right) \Delta \boldsymbol{p}_{ij}\left(t\right) \\ -\gamma \left[\boldsymbol{x}_i\left(t\right) - \overline{\boldsymbol{x}}\left(t - \tau\right)\right],\end{aligned} \tag{4}$$

where $\Delta \boldsymbol{p}_{ij}(t) = \boldsymbol{p}_i(t) - \boldsymbol{p}_j(t) - (\boldsymbol{\delta}_i - \boldsymbol{\delta}_j)$. $\theta$ and $\gamma$ are positive constants. $g_{ij}$ denotes the connection status between two distinct agents $i$ and $j$, i.e., $g_{ij} = 1$ if they are connected and $g_{ij} = 0$ otherwise. There are non-negligible time delays in both the transmission and broadcast of the step 1), so $\tau$ is used to denote the overall time delay. ■

Remark. The term $-\gamma \left[\boldsymbol{x}_i\left(t\right) - \overline{\boldsymbol{x}}\left(t - \tau\right)\right]$ in the control law (4) is introduced by this study, which incorporates a simple global coordination, i.e., the global averaging $\overline{\boldsymbol{x}}\left(t\right)$ specified in (3). It is inspired by the federated learning and optimization in which global averaging is the most commonly used method for global coordination [15], [19].

Moreover, it is always required to specify the initial states for time-delay systems, so the following assumption is made.

Assumption 1 [26]. Multiagent system (1) starts working from $t = 0$, with an initial condition $\overline{\boldsymbol{x}}\left(t\right) =$

$\overline{\boldsymbol{x}}_{init}(t)$ for $t \in [-\tau, 0]$, where $\overline{\boldsymbol{x}}_{init} : [-\tau, 0] \to \mathbb{R}^M$ is a continuous function satisfying

$$\max_{-\tau \le t \le 0} \|\overline{\boldsymbol{x}}_{init}(t)\|_2 < \infty. \tag{5}$$

Remark 1 (Task-Time Early Computability). We will see in the next section (from Theorem 1) that, as early as the system initialization, the server can compute the time that is sufficient for the federated-control procedure to accomplish the task of connecting disconnected agents.

In order to achieve this early computability, we design an initialization procedure as follows.

Initialization Procedure. It is implemented in two steps during the time period $[0, \tau]$:

1) Every agent $i$ calculates $\boldsymbol{x}_i(0)$ and transmits it, together with $\boldsymbol{\delta}_i$, to the sever, allowing the server to compute

$$C^0_{max} = \max_{1 \le i \le N} \|\boldsymbol{x}_i(0) - \overline{\boldsymbol{x}}(0)\|_2. \tag{6}$$

2) For agent pair $(j, i)$ with $\|\boldsymbol{\delta}_i - \boldsymbol{\delta}_j\|_2 < R$, the server computes

$$T^c_{ij} = -\frac{1}{\gamma} \log\left(\frac{R - \|\boldsymbol{\delta}_i - \boldsymbol{\delta}_j\|_2}{2\sqrt{N} C^0_{max}}\right), \tag{7}$$

where $R$ is the communication radius of interagent communication and $T^c_{ij}$ is the time sufficient for the federated-control procedure to connect initially disconnected agents $i$ and $j$. ■

The federated-control and initialization procedures have practical advantages at the cost of a small amount of server-agent communication and extra computation, as explained below.

Remark 2. The federated control allows the early computability of task time at the server, i.e., $T^c_{ij}$ can be computed within the initialization procedure (roughly during the period $[0, \tau]$). On the other hand, in the federated-control and initialization procedures, the transmission and broadcast efforts made by the multiagent system and the server, respectively, are only of the order of $N$. Besides, the server only requires to compute (3) and (6) whose computation complexity are also of the order of $N$.

### B. Interagent Communication

The communication connection between any two agents is supposed to depend on their distance [3]–[5], and the following assumption holds.

Assumption 2. Every agent has a fixed communication radius $R$ [1], [4], [5]. If the distance between two agents is less than $R$, then they are connected, otherwise not connected. To be specific,

$$g_{ij}(t) = \begin{cases} 1, & \text{if } \|\boldsymbol{p}_i(t) - \boldsymbol{p}_j(t)\|_2 < R,\ i \ne j, \\ 0, & \text{if } \|\boldsymbol{p}_i(t) - \boldsymbol{p}_j(t)\|_2 \ge R,\ i \ne j, \\ 0, & \text{otherwise (i.e., } i = j). \end{cases} \tag{8}$$

Denote $\mathcal{V} = \{1, \cdots, N\}$ as the set of $N$ agents. A time-varying graph $\mathcal{G}(t) = (\mathcal{V}, \mathcal{E}(t))$ is used to model the interagent connections (i.e., the connections among the agents), where $\mathcal{E}(t) \in \mathcal{V} \times \mathcal{V}$ is the edge set of paired agents. An edge $(i, j) \in \mathcal{E}(t)$ implies that agent $i$ is connected to agent $j$, leading to $g_{ij}(t) = 1$. Since $(j, i) \in \mathcal{E}(t)$ is equivalent to $(i, j) \in \mathcal{E}(t)$, $\mathcal{G}(t)$ is an undirected graph. Let $\boldsymbol{\mathcal{L}}(t) = [l_{ij}(t)]$ be the Laplacian matrix of the graph $\mathcal{G}(t)$, where $l_{ii}(t) = \sum_{j \ne i} g_{ij}(t)$ and $l_{ij}(t) = -g_{ij}(t)$ for $i \ne j$.

Proposition 1 [21], [24]. The Laplacian matrix $\boldsymbol{\mathcal{L}}(t)$ is symmetric positive semidefinite, such that there exists an orthogonal matrix $\boldsymbol{U}(t)$ to establish

$$\boldsymbol{\mathcal{L}}(t) = \boldsymbol{U}(t)\boldsymbol{\Lambda}(t)\boldsymbol{U}^T(t), \tag{9}$$

where $\boldsymbol{\Lambda}(t) = \operatorname{diag}(\lambda_1(t), \lambda_2(t), \cdots, \lambda_N(t))$ is a diagonal matrix, $\boldsymbol{U}(t)$ can be denoted by $\boldsymbol{U}(t) = \begin{bmatrix} \frac{1}{\sqrt{N}}\mathbf{1}_N & \boldsymbol{Y}(t) \end{bmatrix} \in \mathbb{R}^{N \times N}$, and $\lambda_i(t)$ is the $i$-th smallest eigenvalue of $\boldsymbol{\mathcal{L}}(t)$. Moreover, $\boldsymbol{\mathcal{L}}(t)\mathbf{1}_N = \mathbf{0}$, $\mathbf{1}_N^T \boldsymbol{\mathcal{L}}(t) = 0$, and $\lambda_1(t) \equiv 0$.

Let us also describe the communication topology when the desired formation is achieved by the multiagent system. Let $g^*_{ij}$ be the connection status between agents $i$ and $j$, such that

$$g^*_{ij} = \begin{cases} 1, & \text{if } \|\boldsymbol{\delta}_i - \boldsymbol{\delta}_j\|_2 < R,\ i \ne j, \\ 0, & \text{if } \|\boldsymbol{\delta}_i - \boldsymbol{\delta}_j\|_2 \ge R,\ i \ne j, \\ 0, & \text{otherwise (i.e., } i = j). \end{cases} \tag{10}$$

Define an undirected graph $\mathcal{G}^* = (\mathcal{V}, \mathcal{E}^*)$ to model the interagent connections, where $\mathcal{E}^* \in \mathcal{V} \times \mathcal{V}$ is the edge set of paired agents, and an edge $(j, i) \in \mathcal{E}^*$ means that $g^*_{ij} = 1$, i.e., $\|\boldsymbol{\delta}_i - \boldsymbol{\delta}_j\|_2 < R$. Here $(j, i) \in \mathcal{E}^*$ can be interpreted as that the agents $i$ and $j$ can be connected if the desired shape of formation is achieved. The Laplacian matrix of the graph $\mathcal{G}^*$ is denoted by $\boldsymbol{\mathcal{L}}^* = \left[l^*_{ij}\right]$. Let $\lambda^*_i$ be the $i$-th smallest eigenvalue of $\boldsymbol{\mathcal{L}}^*$ with $1 \le i \le N$, where $\lambda^*_1 \equiv 0$. Assume that there is an orthogonal matrix $\boldsymbol{U}^* = \begin{bmatrix} \frac{1}{\sqrt{N}}\mathbf{1}_N & \boldsymbol{Y}^* \end{bmatrix} \in \mathbb{R}^{N \times N}$, such that $\boldsymbol{\mathcal{L}}^* = \boldsymbol{U}^* \boldsymbol{\Lambda}^* (\boldsymbol{U}^*)^T$.

Under Assumption 2, the communication topology $\mathcal{G}(t)$ of multi-agent system (1) is time-varying. Without loss of generality, we suppose that the number of topology changes during the period from the beginning status to the final one is denoted by $K$, and $\mathcal{G}(t)$ is updated at time instants $T_0, T_1, \cdots, T_K$, where $0 = T_0 < T_1 < \cdots < T_K$. That is, $\mathcal{G}(t) = \mathcal{G}(T_k)$ if $t \in [T_k, T_{k+1})$ with $0 \le k \le K-1$, and $\mathcal{G}(t) = \mathcal{G}(T_K) = \mathcal{G}^*$ if $t \in [T_K, +\infty)$.

## III. Analysis

Having provided the model of the federated-control multiagent system (1), we now state the analytical results showing the behavior of the system (1).

A. Model Transformations

Recalling (2), we express the system (1) as

$$\dot{\boldsymbol{x}}_i(t) = \widetilde{\boldsymbol{u}}_i(t), \tag{11}$$

$$\begin{aligned}\widetilde{\boldsymbol{u}}_i(t) = &-\theta \sum_{j=1}^{N} g_{ij}(t)\left[\boldsymbol{x}_i(t) - \boldsymbol{x}_j(t)\right] \\ &-\gamma\left[\boldsymbol{x}_i(t) - \overline{\boldsymbol{x}}(t-\tau)\right].\end{aligned} \tag{12}$$

Let $\boldsymbol{x}(t) = \begin{bmatrix}\boldsymbol{x}_1^T(t) & \cdots & \boldsymbol{x}_N^T(t)\end{bmatrix}^T$. The system model can be written in a compact form

$$\begin{aligned}\dot{\boldsymbol{x}}(t) = &-\left[(\theta\boldsymbol{\mathcal{L}}(t) + \gamma \boldsymbol{I}_N) \otimes \boldsymbol{I}_M\right]\boldsymbol{x}(t) \\ &+\frac{\gamma}{N}\left(\boldsymbol{1}_N\boldsymbol{1}_N^T \otimes \boldsymbol{I}_M\right)\boldsymbol{x}(t-\tau).\end{aligned} \tag{13}$$

1) Transformation for Distance Analysis: One of our main interests is in verifying that certain disconnected pair of agents within multiagent system (1) can be connected. The verification requires the analysis of distances between agents. We will transform the model (13) into the one that can be used for the distance analysis.

Lemma 1. Let $\boldsymbol{P} = \boldsymbol{I}_N - \boldsymbol{1}_N\left(\boldsymbol{1}_N^T\boldsymbol{1}_N\right)^{-1}\boldsymbol{1}_N^T$ denote the projection matrix onto the nullspace of $\boldsymbol{1}_N^T$. Then

1) $\boldsymbol{P} = \boldsymbol{P}^T = \boldsymbol{P}^2$.
2) $\boldsymbol{1}_N^T\boldsymbol{P} = \boldsymbol{0}_N^T$, or equivalently, $\boldsymbol{P}\boldsymbol{1}_N = \boldsymbol{0}_N$.

Moreover, consider the Laplacian matrix $\boldsymbol{\mathcal{L}}(t) = \boldsymbol{U}(t)\boldsymbol{\Lambda}(t)\boldsymbol{U}^T(t)$, then

$$\boldsymbol{\mathcal{L}}(t) = \boldsymbol{P}\boldsymbol{\mathcal{L}}(t) = \boldsymbol{\mathcal{L}}(t)\boldsymbol{P}, \tag{14}$$

$$\left(\boldsymbol{U}(t)\right)^T\left(\boldsymbol{I}_N - \boldsymbol{D}\right)\boldsymbol{U}(t) = \boldsymbol{P}, \tag{15}$$

where $\boldsymbol{D} = \operatorname{diag}(1, 0, \cdots, 0)$.

Proof: See Appendix A. ■

Defining $\boldsymbol{\xi}(t) = \left(\left(\boldsymbol{U}(t)\right)^T \otimes \boldsymbol{I}_M\right)\left(\boldsymbol{P} \otimes \boldsymbol{I}_M\right)\boldsymbol{x}(t)$, and combining it with the model (13), yields

$$\begin{aligned}\dot{\boldsymbol{\xi}}(t) &= -\left[(\theta\boldsymbol{\Lambda}(t) + \gamma\boldsymbol{I}_N) \otimes \boldsymbol{I}_M\right]\boldsymbol{\xi}(t) \\ &= \left[\operatorname{diag}\left(\mu_1(t), \cdots, \mu_N(t)\right) \otimes \boldsymbol{I}_M\right]\boldsymbol{\xi}(t),\end{aligned} \tag{16}$$

where $\mu_i(t) = -\theta\lambda_i(t) - \gamma$ such that $\mu_i(t) \leq -\gamma$, $1 \leq i \leq N$. The first equality in (16) follows from Lemma 1.

Remark 3. Once the model (16) is derived, the analysis becomes simpler, as (16) is a delay-free linear system. The delay term presented in (13) vanishes in (16) due to the fact

$$\frac{\gamma}{N}\left(\left(\boldsymbol{U}(t)\right)^T \otimes \boldsymbol{I}_M\right)\left(\boldsymbol{P} \otimes \boldsymbol{I}_M\right)\left(\boldsymbol{1}_N\boldsymbol{1}_N^T \otimes \boldsymbol{I}_M\right) \equiv \boldsymbol{O}_{MN}.$$

The model (16) can easily be used to analyze how the distances between agents evolve, because of the property shown in the following lemma.

Lemma 2. Suppose that the state of the system (16) is $\boldsymbol{\xi}(0)$ at $t = 0$. Then

$$\left\|\boldsymbol{p}_i(t) - \boldsymbol{p}_j(t) - (\boldsymbol{\delta}_i - \boldsymbol{\delta}_j)\right\|_2 \leq 2\exp(-\gamma t)\left\|\boldsymbol{\xi}(0)\right\|_2, \tag{17}$$

for all $t \geq 0$.

Proof: See Appendix A. ■

This result implies that $\|\boldsymbol{p}_i(t) - \boldsymbol{p}_j(t) - (\boldsymbol{\delta}_i - \boldsymbol{\delta}_j)\|_2$ decays to zero exponentially fast as $t \to \infty$.

2) Transformation for Velocity Analysis: It is necessary to validate the convergence of the velocities of all agents. The model (13) will be transformed into the one that can be exploited to analyze the velocity behavior of the multiagent system.

Now let us focus on an interval $[T_k, T_{k+1})$ with $k = 0, 1, \cdots, K$, or $[T_k, \infty)$ with $k = K$, in which $\mathcal{G}(t)$ and $\boldsymbol{\mathcal{L}}(t)$ stay constant, i.e., $\mathcal{G}(t) \equiv \mathcal{G}(T_k)$ and $\boldsymbol{\mathcal{L}}(t) \equiv \boldsymbol{\mathcal{L}}(T_k)$. The model (13) can be rewritten as

$$\begin{aligned}\dot{\boldsymbol{x}}(t) = &-\left[(\theta\boldsymbol{\mathcal{L}}(T_k) + \gamma\boldsymbol{I}_N) \otimes \boldsymbol{I}_M\right]\boldsymbol{x}(t) \\ &+\frac{\gamma}{N}\left(\boldsymbol{1}_N\boldsymbol{1}_N^T \otimes \boldsymbol{I}_M\right)\boldsymbol{x}(t-\tau).\end{aligned} \tag{18}$$

We define $\boldsymbol{z}(t) = \left(\boldsymbol{U}^T(T_k) \otimes \boldsymbol{I}_M\right)\boldsymbol{x}(t)$ and have

$$\begin{aligned}\dot{\boldsymbol{z}}(t) = &-\left[(\theta\boldsymbol{\Lambda}(T_k) + \gamma\boldsymbol{I}_N) \otimes \boldsymbol{I}_M\right]\boldsymbol{z}(t) \\ &+\gamma\left(\boldsymbol{D} \otimes \boldsymbol{I}_M\right)\boldsymbol{z}(t-\tau).\end{aligned} \tag{19}$$

This equality holds due to Lemma 1.

As the system model is transformed from (1) to (19), the velocities of all agents, i.e., $\dot{\boldsymbol{p}}_i(t)$, $i = 1, \cdots, N$, can be analyzed by using the property stated in the next lemma.

Lemma 3. After transforming the model from (1) to (19), one have

$$\sum_{i=1}^{N}\left\|\dot{\boldsymbol{p}}_i(t) - \boldsymbol{v}^*\right\|_2^2 = \left\|\dot{\boldsymbol{x}}(t)\right\|_2^2 = \left\|\dot{\boldsymbol{z}}(t)\right\|_2^2. \tag{20}$$

Proof: See Appendix A. ■

To clarify the behaviour of the system (19), let us denote $\boldsymbol{z}(t) = \begin{bmatrix}\boldsymbol{z}_1^T(t) & \cdots & \boldsymbol{z}_N^T(t)\end{bmatrix}^T$ and rewrite (19) as

$$\dot{\boldsymbol{z}}_1(t) = -\gamma\boldsymbol{z}_1(t) + \gamma\boldsymbol{z}_1(t-\tau), \tag{21}$$

$$\dot{\boldsymbol{z}}_i(t) = -\left(\theta\lambda_{i,T_K} + \gamma\right)\boldsymbol{z}_i(t), \quad i = 2, \cdots, N \tag{22}$$

On the one hand, as a first-order delay system, (21) is in a simple form, but it cannot be directly analyzed via classical stability tests including the Tsypkin's test and the frequency sweeping test, or via robust stability methods including small $\mu$ theorem, or even via Razumikhin theorem [26]. Because the coefficients of $\boldsymbol{z}_1(t)$ and $\boldsymbol{z}_1(t-\tau)$ in (21) are $-\gamma$ and $\gamma$, respectively, where $|-\gamma/\gamma| = 1$, representing a marginal case that is not covered by most known results [26]. We will analyze the system (21) in Appendix B by using fundamental mathematical tools such as the method of steps and the final value theorem [26], [27]. On the other hand, the analysis of the system (22) is more easy, which is also given in Appendix B.

## B. Main Results

The first theorem provides sufficient conditions of the time needed to connect certain pair of disconnected agents.

Theorem 1. Apply the control law (4) to multiagent system (1). Let Assumptions 1 and 2 hold. Consider a pair of agents $i$ and $j$ that are disconnected at $t = 0$ but with $\|\boldsymbol{\delta}_i - \boldsymbol{\delta}_j\|_2 < R$. If

$$t \geq T_{ij}^c, \tag{23}$$

where $T_{ij}^c$ is defined in (7), then two agents will get connected, i.e., $\|\boldsymbol{p}_i(t) - \boldsymbol{p}_j(t)\|_2 < R$.

Proof: See Appendix B. ■

Theorem 1 states that $t \geq T_{ij}^c$ is sufficient for connecting certain pair of disconnected agents, where the value of $T_{ij}^c$ can be computed by the server during the time period $[0, \tau]$ using our designed initialization procedure.

Remark 4 (Delay Independence). The values of both $T_{ij}^c$ in Theorem 1 is delay independent, while the reason behind can be deduced from Remark 3.

As a byproduct of the proof of Theorem 1 (in Appendix B), the control law (4) results in the convergence of the formation of multiagent system (1); see the corollary below.

Corollary 1. For any pair of agents $i$ and $j$ in multiagent system (1), the control law (4) leads to

$$\lim_{t\to\infty} \|\boldsymbol{p}_i(t) - \boldsymbol{p}_j(t)\|_2 = \|\boldsymbol{\delta}_i - \boldsymbol{\delta}_j\|_2. \tag{24}$$

Proof: See Appendix B. ■

The second theorem of this paper shows the convergence of the velocities of all agents in the system (1) with the control law (4).

Theorem 2. Consider multiagent system (1) using the control law (4). Let Assumptions 1 and 2 hold. For $t \in [0, T_K]$, the following holds

$$\|\dot{\boldsymbol{p}}_i(t)\|_2 < +\infty. \tag{25}$$

Moreover, if $t \in [T_K, \infty)$, then the velocity of every agent converges to $\boldsymbol{v}^*$, i.e.,

$$\lim_{t\to\infty} \dot{\boldsymbol{p}}_i(t) = \boldsymbol{v}^*, \quad 1 \leq i \leq N. \tag{26}$$

Proof: See Appendix B. ■

For the velocity of every agent in multiagent system (1), Theorem 2 first validates the boundness over the time interval $[0, T_K]$ in which the topology varies, and then confirms the convergence with increasing $t$ in the interval $[T_K, \infty)$.

# IV. Simulations

This section presents simulation results illustrating the behaviour of a multiagent system with federated control that aims at connecting disconnected agents. The simulations are conducted in a two dimensional plane, so that we can write $\boldsymbol{\delta}_i = [\delta_{i,1}\ \delta_{i,2}]^T$, $\boldsymbol{p}_i(t) = [p_{i,1}(t)\ p_{i,2}(t)]^T$, and $\dot{\boldsymbol{p}}_i(t) = [\dot{p}_{i,1}(t)\ \dot{p}_{i,2}(t)]^T$, for every agent $i$. There are 16 agents moving from random initial positions, that is, $\boldsymbol{p}_i(0) = \boldsymbol{w}_i$, where $\boldsymbol{w}_i = [w_{i,1}\ w_{i,2}]^T \in \mathbb{R}^2$ whose entries satisfy $w_{i,m} \sim \mathcal{N}(0, 80^2)$. Suppose that the control law (4) uses the parameters $\theta = 1$ and $\gamma = 2$, with the desired velocity $\boldsymbol{v}^* = [5\,20]^T$. Let the connection radius $R = 43$. The case of interest is depicted in Fig. 3.

Fig. 4 shows the convergence behaviour of $\|\boldsymbol{p}_i(t) - \boldsymbol{p}_j(t)\|_2$ with different $\tau$, when Assumption 1 holds. Agent pairs $(14, 16)$ and $(15, 16)$ are considered, noting that $\|\boldsymbol{\delta}_{14} - \boldsymbol{\delta}_{16}\|_2 = 40$ and $\|\boldsymbol{\delta}_{15} - \boldsymbol{\delta}_{16}\|_2 = 50$. We can observe from Fig. 4 that, as $t$ increases,

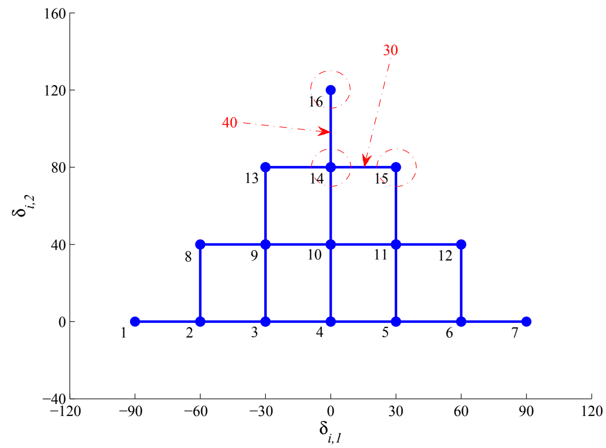


Fig. 3. The desired formation shape determined by $\boldsymbol{\delta}_i$, $1 \leq i \leq 16$, and the corresponding communication graph $\mathcal{G}^*$, where the connection radius $R = 43$. Moreover, $\|\boldsymbol{\delta}_{14} - \boldsymbol{\delta}_{15}\|_2 = 30$, $\|\boldsymbol{\delta}_{14} - \boldsymbol{\delta}_{16}\|_2 = 40$, and $\|\boldsymbol{\delta}_{15} - \boldsymbol{\delta}_{16}\|_2 = 50$.

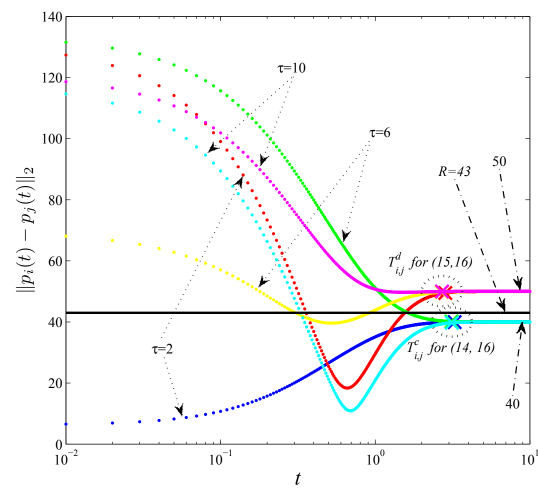


Fig. 4. Convergence curves of the distances between agents $i$ and $j$, i.e., $\|\boldsymbol{p}_i(t) - \boldsymbol{p}_j(t)\|_2$, as $t$ increases, for $\tau = 2$, 6, and 10, where agent pairs $(14, 16)$ and $(15, 16)$ are chosen as examples. The $\times$ markers represent $T_{ij}^c$ and $T_{ij}^d$, respectively, for the cases $\|\boldsymbol{p}_i(T) - \boldsymbol{p}_j(T)\|_2 < R$ and $\|\boldsymbol{p}_i(T) - \boldsymbol{p}_j(T)\|_2 \geq R$.

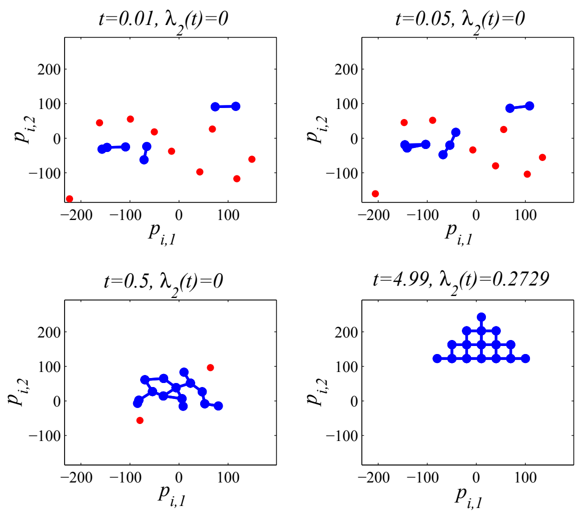


Fig. 5. Snapshots of the formation shape and the communication graph $\mathcal{G}(t)$ at $t = 0.01, 0.05, 0.5$, and 4.99. For each case, the value of $\lambda_2(t)$ is also provided.

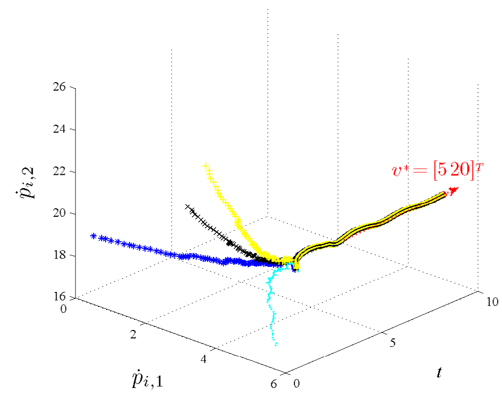


Fig. 6. Convergence curves of the velocities of agents, i.e., $\dot{\boldsymbol{p}}_i(t) = [\dot{p}_{i,1}(t)\ \dot{p}_{i,2}(t)]^T$, as $t$ increases, where agents 1, 5, 9, and 16 are considered. One curve corresponds to one agent.

$\|\boldsymbol{p}_i(t) - \boldsymbol{p}_j(t)\|_2 \rightarrow \|\boldsymbol{\delta}_i - \boldsymbol{\delta}_j\|_2$. This is in accordance with the analytical result of Corollary 1. More importantly, as $\|\boldsymbol{\delta}_{14} - \boldsymbol{\delta}_{16}\|_2 < R = 43$, we see that $\|\boldsymbol{p}_{14}(t) - \boldsymbol{p}_{16}(t)\|_2$ converges to be less than $R$ at some time $t \leq T_{ij}^c$ in every case. This observation can be interpreted as that, as long as $t \geq T_{ij}^c$, one should always have $\|\boldsymbol{p}_i(t) - \boldsymbol{p}_j(t)\|_2 < R$ for two agents $i$ and $j$ with $\|\boldsymbol{\delta}_i - \boldsymbol{\delta}_j\|_2 < R$, which complies with Theorem 1. On the other hand, as $\|\boldsymbol{\delta}_{15} - \boldsymbol{\delta}_{16}\|_2 \geq R$, we observe that $\|\boldsymbol{p}_{15}(t) - \boldsymbol{p}_{16}(t)\|_2$ converges to be larger than $R$ at some time $t \leq T_{ij}^d$ in every case.

To see the effectiveness of the control law (4), we provide four snapshots of the formation shape and $\mathcal{G}(t)$ at $t = 0.01, 0.05, 0.5$, and 4.99 in Fig. 5. One can find that $\mathcal{G}(t)$ is not connected at $t = 0.01, 0.05$, and 0.5, while it becomes connected at $t = 4.99$ such that $\lambda_2(4.99) = 0.2729$. Typical behavior of agents' velocities, i.e., $\dot{\boldsymbol{p}}_i(t)$, is plotted in Fig. 6. It can be seen that all curves of $\dot{\boldsymbol{p}}_i(t)$ approach the desired velocity $\boldsymbol{v}^*$. In summary, Fig. 5 visualizes the analytical results of Theorem 1 and Corollary 1, while Fig. 6 verifies Theorem 2.

## V. Conclusion

This study develops the federated-control technique for connecting disconnected agents in multiagent systems. When investigating how the technique exactly works, we derive the close-form expression of the time sufficient to connect disconnected agents, which is readily computable as early as the system initialization and also delay independent.

In general, the federated-control concept can potentially be applied to the emerging fields of cellular-connected UAVs and cloud-robotics systems that allow swarming UAVs and robots, respectively, to offload their computing and controlling tasks to centralized severs to enhance the capacities [22], [23]. Also, the federated-control technique is applicable to unmanned surface vehicle (USV) systems sailing the oceans, which are connected to control centers via the space-air-ground integrated network. However, our work is just a first step in the direction of federated control, while extensions of analysis to multiagent systems with nonlinear, noisy, and communication-limited control laws, and conducting research in conjunction with additional multiagent control goals (such as path planning, and collision/obstacle avoidance), are meaningful future works.

## Appendix A: Proofs of Used Lemmas

*Proof of Lemma 1:* The results can be verified by doing simple matrix multiplications. Note that the nullspace of $\mathbf{1}_N^T$ consists of all solutions $\boldsymbol{s}$ to $\mathbf{1}_N^T \boldsymbol{s} = 0$, and the projection matrix $\boldsymbol{P}$ projects any vector $\boldsymbol{a} \in \mathbb{R}^N$ to the nullspace of $\mathbf{1}_N^T$, since $\mathbf{1}_N^T(\boldsymbol{P}\boldsymbol{a}) = 0$ [25]. ■

*Proof of Lemma 2:* By definition, we have $\|\boldsymbol{\xi}(t)\|_2^2 = \|(\boldsymbol{P} \otimes \boldsymbol{I}_M)\,\boldsymbol{x}(t)\|_2^2 = \|\boldsymbol{x}(t)\|_2^2 = \sum_{i=1}^N \|\boldsymbol{x}_i(t) - \overline{\boldsymbol{x}}(t)\|_2^2$. Norm inequalities give rise to

$$\begin{aligned}\left(1/\sqrt{N}\right)\|\boldsymbol{\xi}(t)\|_2 &\leq \max_{1\leq i\leq N}\|\boldsymbol{x}_i(t) - \overline{\boldsymbol{x}}(t)\|_2 \\ &\leq \|\boldsymbol{\xi}(t)\|_2 .\end{aligned} \tag{27}$$

Substituting (2) and (3) into (27) results in

$$\|\boldsymbol{p}_i(t) - \boldsymbol{p}_j(t) - (\boldsymbol{\delta}_i - \boldsymbol{\delta}_j)\|_2 \leq 2\,\|\boldsymbol{\xi}(t)\|_2 . \tag{28}$$

On the other hand, denote $\boldsymbol{\xi}(t) = \left[\xi_1(t) \quad \cdots \quad \xi_{MN}(t)\right]^T$. Given the system model (16), use [28, (5.12)] to show that $\xi_{(i-1)N+l}(t) = \exp\left(-(\theta\lambda_i(t) + \gamma)t\right)\xi_{(i-1)N+l}(0)$, where $i = 1, \cdots, N$ and $l = 1, \cdots, M$. Applying the inequalities $\exp(-(\theta\lambda_i(t)+\gamma)t) \le \exp(-\gamma t)$, $i=1,\cdots,N$, to the above equations, yields

$$\|\boldsymbol{\xi}(t)\|_2 \le \exp(-\gamma t)\|\boldsymbol{\xi}(0)\|_2, \quad t \ge 0. \tag{29}$$

The proof is completed by combining (28) and (29). ■

Proof of Lemma 3: First of all, according to the system model (1) with the control input (4) and the system model (11) with the control input (12), respectively, $\boldsymbol{p}_i(t)$ and $\boldsymbol{x}_i(t)$ are continuously differentiable. From (2), we can deduce that $\dot{\boldsymbol{p}}_i(t)-\boldsymbol{v}^* = \dot{\boldsymbol{x}}_i(t)$. Then, (18) and (19) states that $\boldsymbol{z}(t) = \left(\boldsymbol{U}^T(T_k)\otimes \boldsymbol{I}_M\right)\boldsymbol{x}(t)$, so $\dot{\boldsymbol{z}}(t) = \left(\boldsymbol{U}^T(T_k)\otimes \boldsymbol{I}_M\right)\dot{\boldsymbol{x}}(t)$ due to the linearity of differential operation. This yields the desired result. ■

## Appendix B: Proofs of Main Results

Proof of Theorem 1: Combine (6) with the first inequality of (27) to show that

$$\|\boldsymbol{\xi}(0)\|_2 \le \sqrt{N}C^0_{max}. \tag{30}$$

By applying the second inequality of (27) to (17), we get

$$\|\boldsymbol{x}_i(t)-\overline{\boldsymbol{x}}(t)\|_2 \le \|\boldsymbol{\xi}(t)\|_2 \le \sqrt{N}C^0_{max}\exp(-\gamma t) \le \epsilon,$$

if $t$ satisfies

$$t \ge -\frac{1}{\gamma}\log\left(\frac{\epsilon}{\sqrt{N}C^0_{max}}\right). \tag{31}$$

By norm inequalities, it is convenient to obtain that $\|\boldsymbol{p}_i(t)-\boldsymbol{p}_j(t)-(\boldsymbol{\delta}_i-\boldsymbol{\delta}_j)\|_2 \le \|\boldsymbol{x}_i(t)-\overline{\boldsymbol{x}}(t)\|_2 + \|\boldsymbol{x}_j(t)-\overline{\boldsymbol{x}}(t)\|_2 \le 2\epsilon$.

Consider multiagent system (1) using the control law (4), and let Assumptions 1 and 2 hold. If (31) holds, then

$$\|\boldsymbol{p}_i(t)-\boldsymbol{p}_j(t)-(\boldsymbol{\delta}_i-\boldsymbol{\delta}_j)\|_2 \le 2\epsilon, \tag{32}$$

with any positive $\epsilon < C^0_{max}$. This implies that, for every positive number $\varepsilon$, there exists a number $t_\varepsilon = -\frac{1}{\gamma}\log\left(\frac{\varepsilon}{2\sqrt{N}C^0_{max}}\right)$, such that $\left|\|\boldsymbol{p}_i(t)-\boldsymbol{p}_j(t)\|_2 - \|\boldsymbol{\delta}_i-\boldsymbol{\delta}_j\|_2\right| \le \varepsilon$ if $t \ge t_\varepsilon$. Use the above result to show that, if $t \ge T^c_{ij}$, $\|\boldsymbol{p}_i(t)-\boldsymbol{p}_j(t)\|_2 < R$, which concludes the proof. ■

Proof of Corollary 1: Letting $\varepsilon$ in (31) be arbitrarily close to zero, (32) yields the corollary. ■

Proof of Theorem 2: Provided that the communication topology of multiagent system (1) is time-varying, the proof includes two aspects.

First, we use the method of steps [26] to investigate whether the velocities of all agents are up-bounded in $[0,\,T_K]$, although the topology is time-varying.

To this end, consider the state of the dynamics system (21) in the time interval $[T_k,\,T_{k+1})$, $0 \le k \le K-1$, and assume that $\boldsymbol{z}_1(t) = \boldsymbol{\phi}_k(t)$ for $t \in [T_k-\tau, T_k]$, where $\boldsymbol{\phi}_k : [T_k-\tau, T_k] \to \mathbb{R}^M$ is a continuous function satisfying

$$\max_{T_k-\tau \le t \le T_k}\|\boldsymbol{\phi}_k(t)\|_2 < \infty. \tag{33}$$

Then if $t \in [T_k, T_k+\tau]$, we get

$$\begin{aligned}\boldsymbol{z}_1(t) &= e^{-\gamma(t-T_k)}\boldsymbol{z}_1(T_k) \\ &\quad + \gamma\int_{T_k}^{t} e^{-\gamma(t-u)}\boldsymbol{z}_1(u-\tau)du,\end{aligned} \tag{34}$$

such that

$$\|\boldsymbol{z}_1(t)\|_2 \le \|\boldsymbol{z}_1(T_k)\|_2 + \gamma\left\|\int_{T_k}^{t} e^{-\gamma(t-u)}\boldsymbol{z}_1(u-\tau)du\right\|_2.$$

The Cauchy-Schwarz-Buniakowsky inequality yields

$$\left\|\int_{T_k}^{t} e^{-\gamma(t-u)}\boldsymbol{z}_1(u-\tau)du\right\|_2^2 \le \tau^2\|\boldsymbol{\phi}(t)\|_c^2. \tag{35}$$

Therefore, the following holds

$$\max_{T_k \le t \le T_k+\tau}\|\boldsymbol{z}_1(t)\|_2 \le (1+\gamma\tau)\|\boldsymbol{\phi}(t)\|_c. \tag{36}$$

Upon obtaining the inequality (36) for $t \in [T_k, T_k+\tau]$, we can compute analogously for $t \in [T_k+\tau, T_k+2\tau]$. Continuing this process for $q$ times, where $q = \lceil (T_{k+1-T_k})/\tau \rceil$, gives rise to [26]

$$\begin{aligned}\max_{T_k \le t \le T_{k+1}}\|\boldsymbol{z}_1(t)\|_2 &\le (1+\gamma\tau)^q \max_{T_k-\tau \le t \le T_k}\|\boldsymbol{\phi}_k(t)\|_2 \\ &< \infty.\end{aligned} \tag{37}$$

The above implies that $\|\boldsymbol{z}_1(t)\|_2$ has a finite upper bound within the time interval $[0,\,T_K]$, under the Assumption 2.

Second, we check whether the velocities of all agents can converge in the time interval $[T_K,\,+\infty)$.

On the one hand, from (21), the Laplace transform of $\boldsymbol{z}_1(t)$ can be obtained as

$$\boldsymbol{Z}_1(s) = \frac{\boldsymbol{\phi}(0)+\gamma e^{-s\tau}\int_{-\tau}^{0} e^{-sv}\boldsymbol{\phi}(v)dv}{s+\gamma-\gamma e^{-s\tau}}, \tag{38}$$

by noting that the Laplace transform of $\boldsymbol{z}_1(t-\tau)$ is $e^{-\tau s}\boldsymbol{Z}_1(s) + e^{-s\tau}\int_{-\tau}^{0} e^{-sv}\boldsymbol{\phi}(v)dv$ [26, (1.9)].

Let $u(t) = \begin{cases} 1, & t \ge 0 \\ 0, & t < 0 \end{cases}$ be the unit-step function, and define

$$\boldsymbol{y}(t) = \dot{\boldsymbol{z}}_1(t)u(t). \tag{39}$$

The Laplace transform of $\boldsymbol{y}(t)$ is expressed by

$$\begin{aligned}\boldsymbol{Y}(s) &= -\gamma\left(1-e^{-s\tau}\right)\boldsymbol{Z}_1(s) + \gamma e^{-s\tau}\int_{-\tau}^{0} e^{-sv}\boldsymbol{\phi}(v)dv \\ &= \frac{-\gamma\left(e^{s\tau}-1\right)\boldsymbol{\phi}(0) + \gamma s\int_{-\tau}^{0} e^{-sv}\boldsymbol{\phi}(v)dv}{se^{s\tau}+\gamma e^{s\tau}-\gamma}.\end{aligned} \tag{40}$$

Applying the final value theorem [27], and taking the limit $s \to 0$ yields

$$\lim_{t\to\infty}\dot{\boldsymbol{z}}_1(t) = \lim_{t\to\infty}\boldsymbol{y}(t) = \lim_{s\to 0}s\boldsymbol{Y}(s) = \boldsymbol{0}_M. \tag{41}$$

On the other hand, based on (22), simple calculations show that

$$\lim_{t\to\infty} \boldsymbol{z}_i(t) = \mathbf{0}_M, \tag{42}$$

for $i = 2, \cdots, N$, as one can have

$$\boldsymbol{z}_i(t) = e^{-\left(\lambda_{i,T_K}+\gamma\right)(t-T_K)}\boldsymbol{z}_{i,T_K}, \tag{43}$$

where $\lambda_{i,T_K} + \gamma > 0$.

Consider the state of the dynamics system (22). Within the time interval $[0, +\infty)$, the differentiation of $\boldsymbol{z}_i(t)$ converges to $\mathbf{0}_M$ for $t \to \infty$, i.e.,

$$\lim_{t\to\infty} \dot{\boldsymbol{z}}_i(t) = \mathbf{0}_M, \quad i = 2, \cdots, N. \tag{44}$$

From (37) and (43), by definition, (25) can be derived. By Lemma 3, we obtain

$$\lim_{t\to\infty} \sum_{i=1}^{N} \|\dot{\boldsymbol{p}}_i(t) - \boldsymbol{v}^*\|_2^2 = 0. \tag{45}$$

The statement (26) of Theorem 2 can finally be verified by norm inequalities. ■


## Acknowledgment

The research in this paper was supported in part by Beijing Natural Science Foundation (grant no. L232046, L202014), in part by National Natural Science Foundation of China (grant no. 62371052, 61971058), in part by Guizhou Science and Technology Support Program (grant no. [2024]YIBAN144), and in part by China National Key R&D Program (grant no. 2022YFB3303700).


## References


[1] Y. Zhang, S. Li, and J. Weng, "Distributed estimation of algebraic connectivity," IEEE Trans. Cybern., vol. 52, no. 5, pp. 3047-3056, Oct. 2022.

[2] L. Sabattini, C. Secchi, and N. Chopra, "Decentralized estimation and control for preserving the strong connectivity of directed graphs," IEEE Trans. Cybern., vol. 45, no. 10, pp. 2273-2286, Oct. 2015.

[3] Z. Kan, E. Doucette, and W. Dixon, "Distributed connectivity preserving target tracking with random sensing," IEEE Trans. Autom. Control, vol. 64, no. 5, pp. 2166-2173, May 2019.

[4] D. Boskos and D. Dimarogonas, "Robustness and invariance of connectivity maintenance control for multiagent systems," SIAM J. Control Optim., vol. 55, no. 3, pp. 1887-1914, 2017.

[5] A. Gasparri, L. Sabattini, and G. Ulivi, "Bounded control law for global connectivity maintenance in cooperative multirobot systems," IEEE Trans. Robot., vol. 33, no. 3, pp. 700-717, Jun. 2017.

[6] Y. Cao, W. Ren, D. Casbeer, and C. Schumacher, "Finite-time connectivity-preserving consensus of networked nonlinear agents with unknown Lipschitz terms," IEEE Trans. Autom. Control, vol. 61, no. 6, pp. 1700-1705, 2016.

[7] M. Siami and N. Motee, "Growing linear dynamical networks endowed by spectral systemic performance measures," IEEE Trans. Autom. Control, vol. 63, no. 7, pp. 2091-2106, Jul. 2018.

[8] Y. Kim, "Bisection algorithm of increasing algebraic connectivity by adding an edge," IEEE Trans. Autom. Control, vol. 55, no. 1, pp. 170-174, Jan. 2010.

[9] R. Khodayi-mehr, Y. Kantaros, and M. Zavlanos, "Distributed state estimation using intermittently connected robot networks," IEEE Trans. Robot., vol. 35, no. 3, pp. 709-724, Jun. 2019.

[10] R. Aragues, D. Dimarogonas, P. Guallar, and C. Sagues, "Intermittent connectivity maintenance with heterogeneous robots," IEEE Trans. Robot., vol. 37, no. 1, pp. 225-245, Feb. 2021.

[11] L. Gupta, R. Jain, and G. Vaszkun, "Survey of important issues in UAV communication networks," IEEE Commun. Surveys Tuts., vol. 18, no. 2, pp. 1123-1152, Secondquarter 2016.

[12] R. Qian, Z. Duan, Y. Qi, T. Peng, and W. Wang, "Identifying disconnected agents in multiagent systems via external estimators," IEEE Trans. Cybern., vol. 54, no. 2, pp. 1011-1023, Feb. 2024.

[13] J. Liu, Y. Shi, Z. Fadlullah, and N. Kato, "Space-air-ground integrated network: A survey," IEEE Commun. Surveys Tuts., vol. 20, no. 4, pp. 2714-2741, Fourthquarter 2018.

[14] A. Farjadian, B. Thomsen, A. Annaswamy, and D. Woods, "Resilient flight control: An architecture for human supervision of automation," IEEE Trans. Control Syst. Technol., vol. 29, no. 1, pp. 29-42, Jan. 2021.

[15] H. McMahan et al., "Communication-efficient learning of deep networks from decentralized data," in Proc. 20th Int. Conf. Artificial Intelligence and Statistics, pp. 1273-1282, 2017.

[16] T. Li, A. Sahu, A. Talwalkar, and V. Smith, "Federated learning: Challenges, methods, and future directions," IEEE Signal Process. Mag., vol. 37, no. 3, pp. 50-60, May 2020.

[17] H. Yang, Z. Liu, T. Quek, and H. Poor, "Scheduling policies for federated learning in wireless networks," IEEE Trans. Commun., vol. 68, no. 1, pp. 317-333, Jan. 2019.

[18] K. Chakrabarti, N. Gupta, and N. Chopra, "Robustness of iteratively pre-conditioned gradient-descent method: The case of distributed linear regression problem," in Proc. 2021 ACC, pp. 2248-2253, 2021.

[19] T. Li et al., "Federated optimization in heterogeneous networks," in Proc. MLSys 2020, pp. 429-450, 2020.

[20] R. Qian, Y. Qi, Y. Xue, T. Zhou, and J. Zhang, "Federated consensus-based algorithm for stable recovery of sparse signals," IEEE Trans. Veh. Technol., vol. 72, no. 12, pp. 15719-15731, Dec. 2023.

[21] Z. Li and J. Chen, "Robust consensus of linear feedback protocols over uncertain network graphs," IEEE Trans. Autom. Control, vol. 62, no. 8, pp. 4251-4258, Aug. 2017.

[22] M. Afrin, J. Jin, A. Rahman, A. Rahman, J. Wan, and E. Hossain, "Resource allocation and service provisioning in multi-agent cloud robotics: A comprehensive survey," IEEE Commun. Surveys Tuts., vol. 23, no. 2, pp. 842-870, Secondquarter 2021.

[23] H. Wang et al., "Survey on unmanned aerial vehicle networks: A cyber physical system perspective," IEEE Commun. Surveys Tuts., vol. 22, no. 2, pp. 1027-1070, Secondquarter 2020.

[24] C. Godsil and G. Royle, Algebraic Graph Theory. New York, USA: Springer, 2001.

[25] G. Strang, Introduction to Linear Algebra. USA: Wellesley-Cambridge Press, 4th ed., 2009.

[26] K. Gu, V. Kharitonov, and J. Chen, Stability of Time-Delay Systems. USA: Birkhauser, 1st ed., 2003.

[27] G. Franklin, J. Powell, and A. Emami-Naeini, Feedback Control of Dynamic Systems. USA: Pearson Education, 7th ed., 2014.

[28] C. Chen, Linear System Thoery and Design. USA: Oxford Univ. Press, 3rd ed., 1999.